Hindawi Publishing Corporation
Journal of Chemistry
Volume 2013, Article ID 640913, 7 pages
http://dx.doi.org/10.1155/2013/640913

Research Article

Acylation Modification of *Antheraea pernyi* Silk Fibroin Using Succinic Anhydride and Its Effects on Enzymatic Degradation Behavior

Xiufang Li, Ceng Zhang, Lingshuang Wang, Caili Ma, Weichao Yang, and Mingzhong Li

National Engineering Laboratory for Modern Silk, College of Textile and Clothing Engineering, Soochow University, No. 199 Ren'ai Road, Industrial Park, Suzhou, Jiangsu 215123, China

Correspondence should be addressed to Mingzhong Li; mzli@suda.edu.cn

Received 18 December 2012; Revised 27 April 2013; Accepted 8 May 2013

Academic Editor: Debora M. Martino

The degradation rate of tissue engineering scaffolds should match the regeneration rate of new tissues. Controlling the degradation behavior of silk fibroin is an important subject for silk-based tissue engineering scaffolds. In this study, *Antheraea pernyi* silk fibroin was successfully modified with succinic anhydride and then characterized by zeta potential, ninhydrin method, and FTIR. *In vitro*, three-dimensional scaffolds prepared with modified silk fibroin were incubated in collagenase IA solution for 18 days to evaluate the impact of acylation on the degradation behavior. The results demonstrated that the degradation rate of modified silk fibroin scaffolds was more rapid than unmodified ones. The content of the β-sheet structure in silk fibroin obviously decreased after acylation, resulting in a high degradation rate. Above all, the degradation behavior of silk fibroin scaffolds could be regulated by acylation to match the requirements of various tissues regeneration.

1. Introduction

Antheraea pernyi (A. pernyi) silk, one of the two most extensively applied silk species in industry, is the natural protein fiber excreted and spun by the wild silkworm. Compared with *Bombyx mori* silk fibroin, *A. pernyi* silk fibroin (*Ap*-SF) contains abundant tripeptide sequences of arg-gly-asp (RGD), known as a cell adhesive site for mammalian cell culture [1]. Considering this, interest has been arisen into the use of *Ap*-SF as a starting material for advanced biomedical applications such as cell culture substrates, surgical mending materials, and tissue engineering scaffolds [2–5]. *Ap*-SF scaffolds used in tissue engineering should possess the corresponding degradation rates with different tissues such as bone, tendons, vessels or skin [6–9]. Therefore, it's still a primary target to regulate the degradation rate of the scaffolds to facilitate the formation of new tissues in tissue engineering.

Secondary structure is critical to the degradation rate of *Ap*-SF scaffolds [9–12], and the degradation conditions also contribute to it [13–15]. Previous studies have showed that protease preferentially attacks the amorphous region of silk fibroin rather than the crystalline region. In crystalline region, the chain segments stretched sufficiently, bonded tightly, and arranged parallelly to each other which were dependent on the quantity of hydrogen bonds [12, 14]. It is probable to regulate the degradation rate of silk fibroin scaffolds by controlling the content of β-sheet structure. The following methods have been studied to change the degradation rates of *Ap*-SF scaffolds previously. Gamma radiation could accelerate biodegradation [16], but high doses of irradiation undoubtedly would damage the covalent bond of fibroin macromolecules. The degradation rate of *Ap*-SF scaffolds could also be affected by means of modulating pore structure, postprocessing conditions, and blending [6, 17]. Besides, *in vivo* study indicated that the degradation behavior of *Ap*-SF scaffolds was affected by the morphological and structural features because of different preparation processes [18]. Furthermore, chemical cross-linking could change the degradation rate of *Ap*-SF scaffolds. In fact, it has been reported that the biodegradation rate was inversely proportional to the cross-linking degree of *Ap*-SF films [19]. To further control the degradation behavior to meet various

tissues regeneration requirements, it is essential to explore potential factors that affect the degradation of *Ap*-SF scaffolds and to search new approaches to control their degradation behavior.

Acylation modification is an effective approach to regulate the conformation of proteins, especially succinylation [20–22]. Bean protein modified by the succinylation had a significant change in conformational and physicochemical properties including protein solubility, emulsifying, and gelling properties due to the increase of electrostatic repulsion [20].

The hypothesis in the present study is that the acylation modification of *Ap*-SF with succinic anhydride could enhance the electrostatic repulsion and steric hindrance between chain segments and prevent the formation of vast hydrogen bonds and β-sheet conformation, so as to accelerate the degradation of *Ap*-SF scaffold. To confirm this hypothesis, succinic anhydride was reacted with the side chains of *Ap*-SF, and the modified *Ap*-SF carrying more negative charges was used to prepare three-dimensional porous scaffolds, and the molecular conformation of modified *Ap*-SF was also discussed in this study. Furthermore, the effect of conformational changes aroused by acylation on the degradation behavior of *Ap*-SF scaffolds was investigated via *in vitro* degradation experiments.

2. Materials and Methods

2.1. Preparation of Ap-SF Solution. *Ap*-SF solution was prepared following the procedure described previously [23]. Briefly, *A. pernyi* silk fibers were degummed three times in 4.7 mM Na_2CO_3 solution at 98–100°C for 30 min. After rinsing and air drying at 60°C, the pure *Ap*-SF fibers were dissolved in melted calcium nitrate 4 hydrate (bath ratio 1 : 1) at 105°C for 5 h. The thermal decomposition temperature of *Ap*-SF is in the range of 220 to 400°C [5], so it did not char during the course of heating. The cooled *Ap*-SF solution was dialyzed (MWCO 9000) against deionized water for 4 days to obtain the *Ap*-SF solution with a concentration of about 2.4 wt.%.

2.2. Acylation Modification of Ap-SF Solution. The *Ap*-SF solution was diluted to 2.0 wt.% with deionized water. 50 mL *Ap*-SF solution (2.0 wt.%) was stirred in ice bath and gradually mixed with succinic anhydride (Sigma-Aldrich) at 1, 2, 3, 4, 5, 10, and 20% of *Ap*-SF weight, respectively. The pH was maintained at 7.5–8.5 using NaOH solution during the reaction. After the pH was balanced at ~8.0, the solution was kept for another 1 h to react completely. Finally, the modified *Ap*-SF solution was dialyzed against deionized water at 4°C for 24 h.

2.3. Measurement of Zeta Potential. After adjusting the pH value to about 7, the zeta potential of *Ap*-SF solution was determined at 25°C by using a zeta potential analyzer (Malvern Zetasizer Nano ZS90).

2.4. Measurement of Acylation Degree. The unreacted amino groups were determined according to Lamothe's ninhydrin method [24]. Briefly, 1 mL of 1 w/v% modified *Ap*-SF solution was mixed with the same volume of 2 w/v% ninhydrin (Sigma-Aldrich) aqueous solution and stirred slowly in water bath at 100°C for 5 min. 5 mL of distilled water was added after cooling. To avoid *Ap*-SF arising condensation or even transforming to gel, the pH was kept at 7-8 by NaOH solution during the reaction, then the optical density (OD) value at 570 nm was obtained by using an ultraviolet spectrophotometer (UV-Vis, Hitachi UV-3010, Japan). 2 w/v% ninhydrin aqueous solution was used to obtain a standard curve. Acylation degree was expressed as the percentage of the difference between the OD value of modified *Ap*-SF solution and the OD value of unmodified *Ap*-SF solution relative to the OD value of unmodified *Ap*-SF solution.

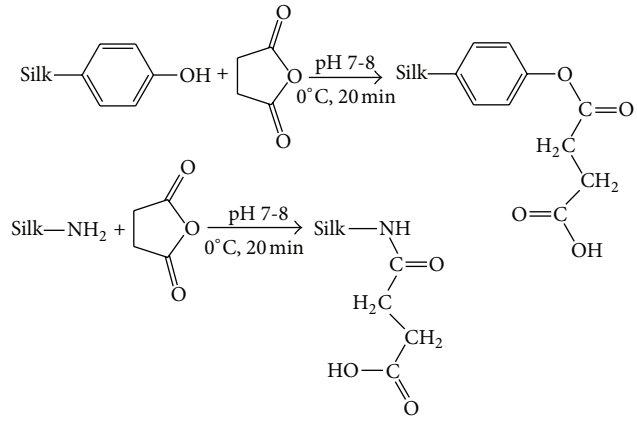

Figure 1: Some potential reactions between *Ap*-SF and succinic anhydride.

2.5. Preparation of Ap-SF Scaffolds. *Ap*-SF solution was stirred slowly in ice bath, and 2-morpholinoethanesulfonic acid/N-hydroxysuccinimide/1-ethyl-3-(3-dimethylaminopropyl) carbodiimide hydrochloride (MES/NHS/EDC, 20/10/20 wt.%) was successively added to crosslink *Ap*-SF. After reacting for 4 h, the pH was adjusted to 7 by using NaOH solution. After vacuum treatment for 3 min, the mixed solution was poured into a stainless steel vessel (25 × 16 cm) to make a 3 mm thick solution then frozen at −40°C for 6 h. Subsequently, it was lyophilized by a Virtis Genesis 25-LE Freeze Dryer for about 36 h to obtain the *Ap*-SF scaffolds.

2.6. Enzymatic Degradation of Ap-SF Scaffolds. Collagenase IA (Sigma-Aldrich) was dissolved in 0.05 M sodium phosphate buffer solution (PBS, pH 7.4) to prepare the enzyme solution (1.0 U/mL). The lyophilized *Ap*-SF scaffolds (not rinsed with water) were cut into 3 × 3 cm squares and weighed. The samples were incubated in 1.0 U/mL collagenase IA solution at 37°C (bath ratio 1 : 50). After 1, 3, 6, 12, and 18 days, 5 squares were collected from each group, and the enzyme solution containing the degradation products was replaced with fresh enzyme solution every 3 days. Groups of samples were rinsed with deionized water and then lyophilized. Quantitative changes were expressed

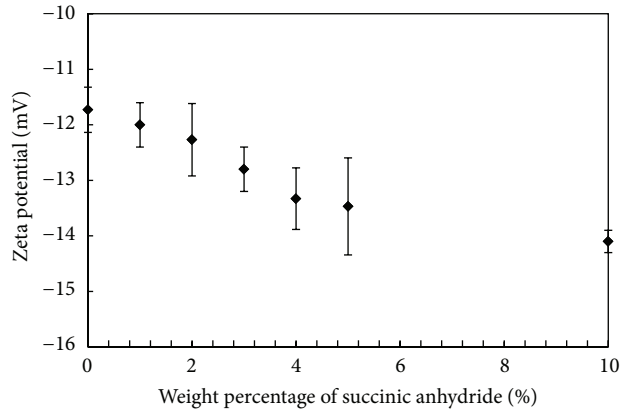

Figure 2: The influence of succinic anhydride weight percentage against *Ap*-SF on zeta potential.

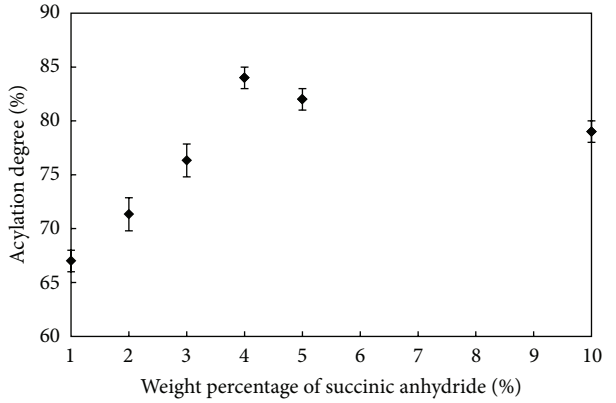

Figure 3: The influence of succinic anhydride weight percentage against *Ap*-SF on acylation degree.

as the percentage of weight retained relative to the initial dry weight. $P < 0.05$ was considered to be statistically significant (t-test). SPSS version 16.0 (SPSS Inc., Chicago, Illinois) software was used for analyses.

2.7. Fourier Transform Infrared Spectroscopy (FTIR). FTIR analysis was performed with a Nicolet 5700 spectrometer to obtain the FTIR spectra of *Ap*-SF scaffolds. The contents of different secondary structures were calculated by infrared spectra in previous studies [25, 26]. Compared with amide II and III, the amide I (1595–1720 cm^{-1}) of *Ap*-SF was more sensitive during degradation [11], so it was selected and analyzed by PeakFit v4.12 software (Systat Software Inc., USA) to obtain the percentage of different secondary structures in *Ap*-SF scaffolds.

2.8. Scanning Electron Microscopy (SEM). The appearance morphology of samples after degradation in collagenase IA solution for different days was examined by using SEM (Hitachi S-4800, Japan).

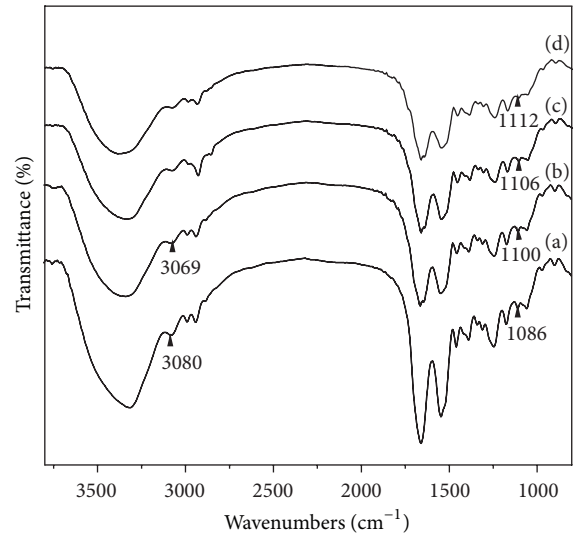

Figure 4: The FTIR spectra of the *Ap*-SF scaffolds (a) unmodified; (b)–(d) modified by 4, 10, and 20 wt.% succinic anhydride, respectively.

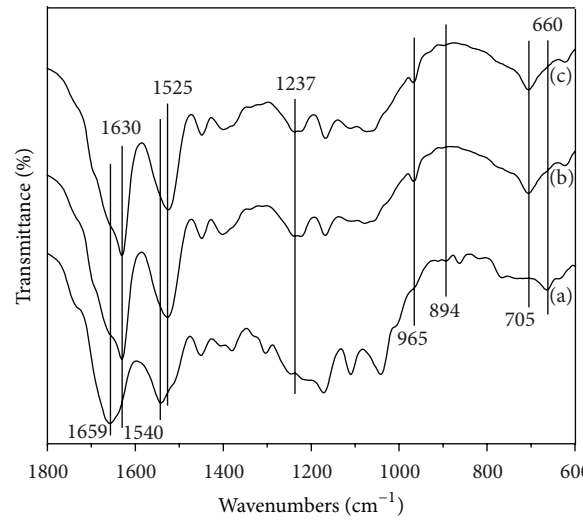

Figure 5: The FTIR spectra of modified *Ap*-SF scaffolds after enzymatic degradation for (a) 0 day; (b) 6 days; (c) 18 days.

3. Results and Discussion

3.1. Acylation Modification of Ap-SF. As illustrated in Figure 1, the potential acylation reactions of *Ap*-SF involved nucleophilic addition reactions between succinic anhydride and amino side chains of lysine residues (0.3 mol% in *Ap*-SF) or phenolic hydroxyl groups of tyrosine (4.7 mol% in *Ap*-SF). The reaction rates of homologous nucleophilic groups depended on the attack rates of the groups, which were inversely proportional to their pK values. The amino side chains of lysine had a lower pK value than the phenolic hydroxyl groups of tyrosine, so the acylation reactions occurred on lysine residues more easily.

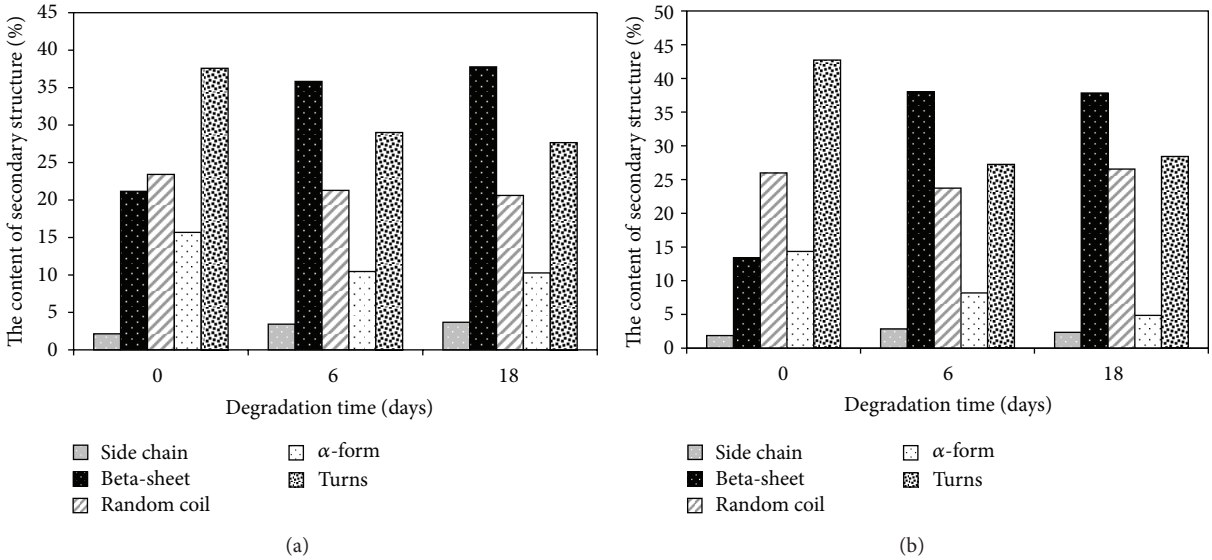

Figure 6: The content of secondary structure of scaffolds after enzymatic degradation for 0, 6, and 18 days (a) unmodified; (b) modified.

3.2. Zeta Potential of Modified Ap-SF. As shown in Figure 2, the zeta potential of *Ap*-SF solutions decreased as succinic anhydride weight increased. Before 4 wt.% of succinic anhydride against *Ap*-SF, the zeta potential reduced gradually from −11.7 to −13.3 mV at a relatively rapid rate. From 4 wt.% to 10 wt.%, the continuous slow decrease was conducted to about −14.1 mV. According to the potential reactions shown in Figure 1, the amino side chains with positive charge and the phenolic hydroxyl groups were replaced by the carboxyl groups with negative charge, resulting in the decrease of zeta potential. These results suggested that *Ap*-SF had reacted with succinic anhydride.

3.3. Acylation Degree of Modified Ap-SF. In Figure 3, the acylation degree of *Ap*-SF changed as succinic anhydride weight increased. Before 4 wt.% of succinic anhydride against *Ap*-SF, the acylation degree increased gradually, reached about 84% at 4 wt.% and it began to reduce slightly after 4 wt.%. Acylation degree reflected the extent of reaction between amino side chains of lysine and succinic anhydride. Compared to tyrosine residues, lysine reacted more easily with succinic anhydride. However, the reaction between succinic anhydride and lysine was restrained after 4 wt.% (Figure 3) due to the competition of the reaction between tyrosine residues and succinic anhydride which resulted in the continuous increase of negative charge and decrease of zeta potential in *Ap*-SF (Figure 2). The 4 wt.% of succinic anhydride was selected to investigate the degradation behavior of modified *Ap*-SF scaffolds in this study.

3.4. FTIR Spectra of Ap-SF Scaffolds. Figure 4 showed the FTIR spectra of scaffolds from modified and unmodified *Ap*-SF. The peak at 1086 cm^{-1} (Figure 4(a)) shifted to the peak at 1100 cm^{-1} (Figure 4(b)), 1106 cm^{-1} (Figure 4(c)), and 1112 cm^{-1} (Figure 4(d)), respectively. It was previously reported that the absorption peak at 1250~1000 cm^{-1} could be assigned to the C–O–H stretching vibrations of tyrosine residues, and stretching vibrations of C–O–C structure had two absorption bands at 1330~1050 cm^{-1} [27]. The electron-withdrawing effect (-I effect) caused by the stronger electronegativity of C–O–C compared to C–O–H led to the stretching vibrational changes of C–O structure, and the changes caused violet shifts from 1086 to 1100–1112 cm^{-1}. This suggested that succinic anhydride had reacted with the phenolic hydroxyl groups of tyrosine residues. On the other hand, the N-H bend peak shifted from 3080 to 3069 cm^{-1}, suggesting that succinic anhydride reacted with amino side chains in *Ap*-SF. The results demonstrated that *Ap*-SF solution was successfully modified by succinic anhydride.

3.5. Structural Changes in Ap-SF Scaffolds during Enzymatic Degradation. As shown in Figure 5, the characteristic peaks of α-helix at 1659 and 894 cm^{-1} and the peaks of random coil at 1540 and 660 cm^{-1} disappeared, while the peaks at 1630, 1525, 705, and 965 cm^{-1} appeared after degradation for 6 days and 18 days, indicating that the content of random coil and α-helix decreased and the content of β-sheet increased during degradation. As shown in Figure 6, the β-sheet content of modified *Ap*-SF scaffolds (13.4%) was less than unmodified ones (21.2%) before degradation. The negative charge of modified *Ap*-SF increased comparing with unmodified ones. The electrostatic and steric-hindrance effects increased among macromolecules of modified *Ap*-SF due to the changes of side chains, so it was more difficult to form the β-sheet structure in the lyophilization process. From Figure 6(a), the content of the random coil decreased from 23.4% to 21.3%, and the content of the β-sheet increased from 21.2% to 35.8% in unmodified *Ap*-SF scaffolds after degradation for 6 days.

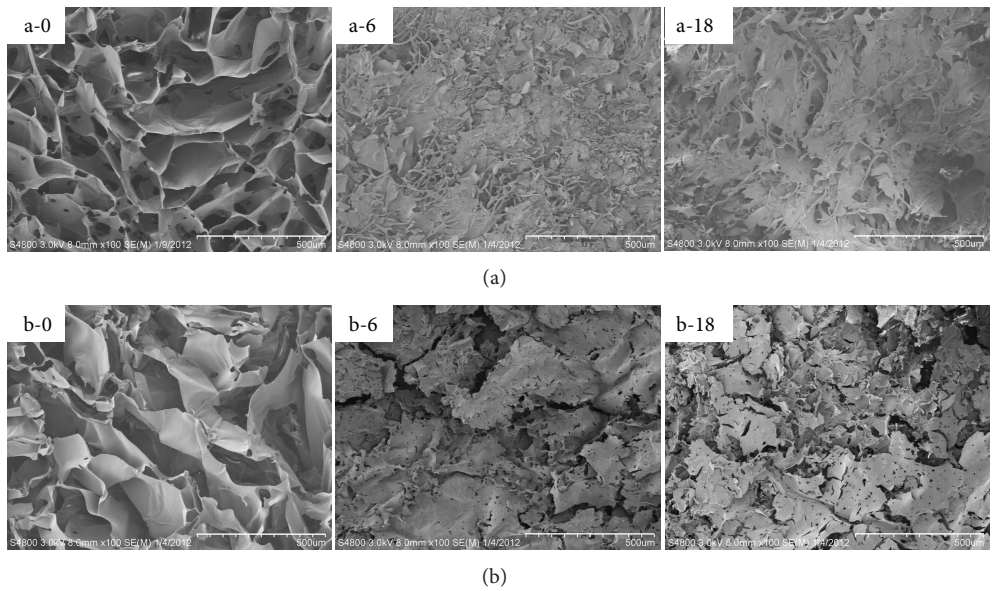

Figure 7: SEM images of scaffolds incubated in the enzymatic solution for 0, 6, and 18 days (a) unmodified; (b) modified (Scale bars = 500 μm).

After 18 days, the content of the random coil reduced to 20.6%, while the content of the β-sheet increased to 37.8% in the residual scaffolds. In Figure 6(b), the content of the random coil decreased from 26.0% to 23.7%, while the content of the β-sheet increased from 13.4% to 38.0% in modified *Ap*-SF scaffolds after 6-day degradation. After 18 days, the content of the random coil reduced to 26.5%, while the content of the β-sheet increased to 37.8% in the residual scaffolds. These data were consistent with our previous observations in the degradation behavior of SF scaffolds. Owing to the preference attacking of the collagenase IA to the amorphous region of silk fibroin, the content of the random coil decreased and the content of the β-sheet structure relatively increased during incubation [12].

3.6. Morphologic Changes during Degradation. The degradation of *Ap*-SF scaffolds for different days in collagenase IA solution was examined by SEM (Figure 7). *Ap*-SF scaffolds were full of pores, and the pore shape was irregular polygon shape. After degradation for 18 days, the pore structure began to collapse, but partial integrity could be maintained. However, modified ones could not retain the original morphology and was fully collapsed to sheets after degradation for 18 days. This indicated that acylation modification could promote degradation of *Ap*-SF.

3.7. Weight Loss during Degradation. Figure 8 shows the weight loss of *Ap*-SF scaffolds during enzymatic degradation. The *Ap*-SF scaffolds weight was reduced gradually after collagenase IA incubation. The difference of the weight loss between the two scaffolds was significant ($P < 0.05$) on the 12th day, and the difference was more significant ($P < 0.01$) on the 18th day. The weight retention of the modified *Ap*-SF scaffold reduced to 27.5% after 18 days, whereas the unmodified scaffold reduced to 37.8%, reflecting that the degradation of modified *Ap*-SF scaffolds was more rapid than unmodified ones. The acylation modification of *Ap*-SF with succinic anhydride enhanced the electrostatic repulsion and steric hindrance between the chain segments and prevented the formation of vast hydrogen bonds and β-sheet conformation. A lower content of β-sheet structure could lead to a higher degradation rate. Therefore, acylation could accelerate the degradation of *Ap*-SF scaffolds.

4. Conclusions

Antheraea pernyi silk fibroin (*Ap*-SF) was successfully modified with succinic anhydride. As the weight percentage of succinic anhydride approximated to 4 wt.% against *Ap*-SF, acylation degree reached about 84% and zeta potential reduced from −11.7 to −13.3 mV. The β-sheet content of *Ap*-SF scaffolds decreased after acylation, resulting in a higher degradation rate against collagenase IA. Acylation modification could promote the degradation of *Ap*-SF scaffolds. This study developed a new method to regulate the degradation rate of *Ap*-SF scaffolds to meet the requirements of tissue regenerations.

Acknowledgments

The authors thank the College Natural Science Research Project of Jiangsu Province (12KJA 430003), the National Nature Science Foundation of China (30970714), the Key Laboratory Opening Program of Jiangsu Higher Education Institutions (KJS1216), and the Priority Academic Program Development of Jiangsu Higher Education Institutions for

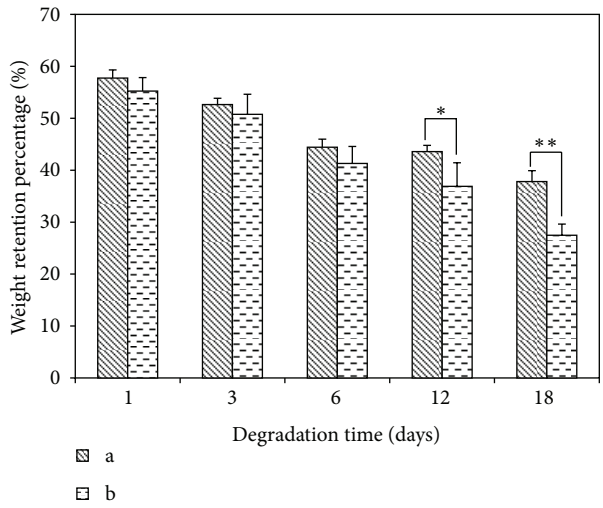

Figure 8: The weight loss of the scaffolds after enzymatic degradation for 1, 3, 6, 12, and 18 days (a) unmodified; (b) modified. $^{*}P < 0.05$, $^{**}P < 0.01$.

the support of this research. They also appreciate the Systat Software Inc providing the PeakFit v4.12 demonstration software in its web site, and the authors used the software to analyze their experimental data during free-trial period.

References

[1] N. Minoura, S. I. Aiba, M. Higuchi, Y. Gotoh, M. Tsukada, and Y. Imai, "Attachment and growth of fibroblast cells on silk fibroin," *Biochemical and Biophysical Research Communications*, vol. 208, no. 2, pp. 511–516, 1995.

[2] C. Fu, D. Porter, X. Chen, F. Vollrath, and Z. Shao, "Understanding the mechanical properties of *Antheraea pernyi* Silka-From primary structure to condensed structure of the protein," *Advanced Functional Materials*, vol. 21, no. 4, pp. 729–737, 2011.

[3] H. Kweon and Y. H. Park, "Dissolution and characterization of regenerated *Antheraea pernyi* silk fibroin," *Journal of Applied Polymer Science*, vol. 82, no. 3, pp. 750–758, 2001.

[4] H. Y. Kweon and Y. H. Park, "Structural and conformational changes of regenerated *Antheraea pernyi* silk fibroin films treated with methanol solution," *Journal of Applied Polymer Science*, vol. 73, no. 14, pp. 2887–2894, 1999.

[5] H. Y. Kweon, I. C. Um, and Y. H. Park, "Thermal behavior of regenerated *Antheraea pernyi* silk fibroin film treated with aqueous methanol," *Polymer*, vol. 41, no. 20, pp. 7361–7367, 2000.

[6] U. J. Kim, J. Park, H. Joo Kim, M. Wada, and D. L. Kaplan, "Three-dimensional aqueous-derived biomaterial scaffolds from silk fibroin," *Biomaterials*, vol. 26, no. 15, pp. 2775–2785, 2005.

[7] O. Hakimi, D. P. Knight, F. Vollrath, and P. Vadgama, "Spider and mulberry silkworm silks as compatible biomaterials," *Composites Part B*, vol. 38, no. 3, pp. 324–337, 2007.

[8] L. S. Nair and C. T. Laurencin, "Biodegradable polymers as biomaterials," *Progress in Polymer Science*, vol. 32, no. 8-9, pp. 762–798, 2007.

[9] Q. Lu, B. Zhang, M. Li et al., "Degradation mechanism and control of silk fibroin," *Biomacromolecules*, vol. 12, no. 4, pp. 1080–1086, 2011.

[10] R. L. Horan, K. Antle, A. L. Collette et al., "*In vitro* degradation of silk fibroin," *Biomaterials*, vol. 26, no. 17, pp. 3385–3393, 2005.

[11] P. Taddei, T. Arai, A. Boschi, P. Monti, M. Tsukada, and G. Freddi, "*In vitro* study of the proteolytic degradation of *Antheraea pernyi* silk fibroin," *Biomacromolecules*, vol. 7, no. 1, pp. 259–267, 2006.

[12] Y. Hu, Q. Zhang, R. You, L. Wang, and M. Li, "The relationship between secondary structure and biodegradation behavior of silk fibroin scaffolds," *Advances in Materials Science and Engineering*, vol. 2012, Article ID 185905, 5 pages, 2012.

[13] T. Arai, G. Freddi, R. Innocenti, and M. Tsukada, "Biodegradation of *Bombyx mori* silk fibroin fibers and films," *Journal of Applied Polymer Science*, vol. 91, no. 4, pp. 2383–2390, 2004.

[14] M. Li, M. Ogiso, and N. Minoura, "Enzymatic degradation behavior of porous silk fibroin sheets," *Biomaterials*, vol. 24, no. 2, pp. 357–365, 2003.

[15] C. Zhao, X. Wu, Q. Zhang, S. Yan, and M. Li, "Enzymatic degradation of *Antheraea pernyi* silk fibroin 3D scaffolds and fibers," *International Journal of Biological Macromolecules*, vol. 48, no. 2, pp. 249–255, 2011.

[16] A. Kojthung, P. Meesilpa, B. Sudatis, L. Treeratanapiboon, R. Udomsangpetch, and B. Oonkhanond, "Effects of gamma radiation on biodegradation of *Bombyx mori* silk fibroin," *International Biodeterioration and Biodegradation*, vol. 62, no. 4, pp. 487–490, 2008.

[17] Z. She, B. Zhang, C. Jin, Q. Feng, and Y. Xu, "Preparation and *In vitro* degradation of porous three-dimensional silk fibroin/chitosan scaffold," *Polymer Degradation and Stability*, vol. 93, no. 7, pp. 1316–1322, 2008.

[18] Y. Wang, D. D. Rudym, A. Walsh et al., "*In vivo* degradation of three-dimensional silk fibroin scaffolds," *Biomaterials*, vol. 29, no. 24-25, pp. 3415–3428, 2008.

[19] Y. Xu, Y. Wang, Y. Jiao, C. Zhang, and M. Li, "Enzymatic degradation properties of silk fibroin film," *Journal of Fiber Bioengineering and Informatics*, vol. 4, no. 1, pp. 35–41, 2011.

[20] S. W. Yin, C. H. Tang, Q. B. Wen, X. Q. Yang, and D. B. Yuan, "The relationships between physicochemical properties and conformational features of succinylated and acetylated kidney bean (*Phaseolus vulgaris* L.) protein isolates," *Food Research International*, vol. 43, no. 3, pp. 730–738, 2010.

[21] S. W. Yin, C. H. Tang, Q. B. Wen, and X. Q. Yang, "Effects of acylation on the functional properties and *In vitro* trypsin digestibility of red kidney bean (*Phaseolus vulgaris* L.) protein isolate," *Journal of Food Science*, vol. 74, no. 9, pp. E488–E494, 2009.

[22] A. C. Hengge and R. L. Stein, "Role of protein conformational mobility in enzyme catalysis: acylation of α-chymotrypsin by specific peptide substrates," *Biochemistry*, vol. 43, no. 3, pp. 742–747, 2004.

[23] W. Tao, M. Li, and C. Zhao, "Structure and properties of regenerated *Antheraea pernyi* silk fibroin in aqueous solution," *International Journal of Biological Macromolecules*, vol. 40, no. 5, pp. 472–478, 2007.

[24] P. J. Lamothe and P. G. McCormick, "Influence of acidity on the reaction of ninhydrin with amino acids," *Analytical Chemistry*, vol. 44, no. 4, pp. 821–825, 1972.

[25] E. Goormaghtigh, J. M. Ruysschaert, and V. Raussens, "Evaluation of the information content in infrared spectra for protein secondary structure determination," *Biophysical Journal*, vol. 90, no. 8, pp. 2946–2957, 2006.

[26] D. M. Byler and H. Susi, "Examination of the secondary structure of proteins by deconvolved FTIR spectra," *Biopolymers*, vol. 25, no. 3, pp. 469–487, 1986.

[27] P. Innocenzi, L. Malfatti, A. Marcelli, and M. Piccinini, "Evaporation-induced crystallization of pluronic F127 studied in situ by time-resolved infrared spectroscopy," *Journal of Physical Chemistry A*, vol. 114, no. 1, pp. 304–308, 2010.